Astrometric detection of trans-Neptunian object (90482) Orcus' satellite Vanth

Aleksandar Cikota

Supervisor: dr.sc. Dejan Vinković

Split, July 2012

Bachelor Thesis in Physics

Department of Physics
Faculty of Natural Sciences and Mathematics
University of Split

Abstract

Relative astrometry of transneptunian object (90482) Orcus along a period of 33 days is presented from more than 180 CCD images acquired by means of a 0.45m f/2.8 telescope on 18 nights. The right ascension residuals of an orbital fit to the astrometric data reveal a periodicity of 9.7 $\pm$ 0.3 days, which is coincident within error bars with the orbital period of the satellite Vanth. The residuals also are correlated with the theoretical positions of the satellite relative to the primary. Therefore the presence of Vanth is unambiguously detected in our astrometry. The oscillation in the residuals is not due to Orcus motion around the barycenter of the system, but due to the photocenter motion of the combined Orcus plus satellite system along an orbital rotation of the satellite. The photocenter motion is much larger than the motion of Orcus around the barycenter and we show here that detecting binaries through a carefully devised astrometric technique is feasible. We discuss the prospects for using the technique to find new binary TNOs and to study already known binary systems with uncertain orbital periods.

Comment: This study was presented at the TNO 2010 conference in Philadelphia, PA by myself and extended with a photometric study of (90482) Orcus published in Ortiz et al. [2011].

Contents

Chapter 1

Background

1.1 Introduction

Trans-Neptunian Objects (TNOs) are important bodies because they are thought to be leftovers from the process of the formation of the solar system and they carry important information about the early stages of the solar system [Morbidelli et al., 2005, Tsiganis et al., 2005, Gomes et al., 2005]. They are also thought to be the parents of the short-period comets [Fernandez, 1980] and therefore a source of objects that eventually can come close to the Sun or to the Earth. Among the TNOs, there are dwarf planets whose study is important per se, but also because they provide a wealth of information about the physical processes that take or took place in the trans-Neptunian Belt. Large TNOs are supposed to retain primordial information about the original spin rate distribution because apparently they are the least collisionally evolved objects [Davis and Farinella, 1997, Benavidez and Campo Bagatin, 2009]. However, some degree of spin evolution owing to tidal interactions in binaries can alter this concept and, Orcus may represent a good example as does Pluto.

The trans-Neptunian object (90482) Orcus (also known as 2004 DW from its provisional designation) is one of the brightest known TNOs discovered so far and possibly one of the largest. Indeed, Orcus qualifies to become a dwarf planet because of its large diameter (D=850$\pm$90 km), which has recently been measured with enough precision by the *Herschel Space Observatory* Lim et al. [2010] and is consistent with *Spitzer* measurements [Stansberry et al., 2008]. It belongs to the plutino dynamical class and it is therefore the largest plutino immediately after Pluto. Besides, Orcus is an interesting object for other reasons: It is known to posses a satellite, Vanth, which orbits Orcus in around 9.5 days and whose orbital plane is almost perpendicular to the line of sight [Brown et al., 2010]. Water ice and perhaps even ammonia has been found on its surface through near infrared spectroscopy [Fornasier et al., 2004, Trujillo et al., 2005, de Bergh et al., 2005, Barucci et al., 2008].

Also, its short term variability was studied in Ortiz et al. [2006] who found a likely rotation period of 10.08 hr (although periods at around 7 hr and 17 hr were also possible). Later, Thirouin et al. [2010] included more data, obtaining a rotation period of 10.47 hr. In both works the variability was very low (≤ 0.04 mag). Other works on the short-term variability of Orcus by Sheppard et al. (2007) and Tegler et al. [2005] failed to find a high amplitude periodicity in Orcus, but those works did not reject the possibility of a lightcurve with an amplitude below 0.06 mag (Sheppard [2007]), which is consistent with the Ortiz et al. (2006) results, and the 0.02mag variability in 7 hours of observation reported by Tegler et al. (2005) is particularly consistent with the Ortiz et al. (2006) and Thirouin et al. (2010) rotational lightcurves.

We intended to check whether the presence of Orcus' satellite could be detected by means of high-precision relative astrometry with respect to background stars in order to test the technique for future detection of new binaries by means of telescopes other than the Hubble Space Telescope (HST). Besides, the technique might help in determining the orbital periods of the known binaries whose orbits are very uncertain. Because Orcus' satellite separation is around 0.3 arcsec, with a small mass ratio, these observations seem challenging, but because Orcus is also among the brightest TNOs, we decided to test the technique with a small telescope (which can easily provide the needed large field of view).

In this work we report the results from our long astrometry runs on Orcus. In the first section of the paper we describe the observations and the applied basic image reductions. A second section is devoted to showing the results and their analysis, a discussion section follows and finally a conclusions section summarizes our main findings.

Chapter 2

Research area

2.1 Trans-Neptunian Objects

There are millions of icy bodies hidden in the dark beyond the orbit of Neptune. The Trans-Neptunian objects are too small and distant and have been undetected until very recently. Pluto was the first trans-Neptunian object to be discovered in 1930 by Clyde W. Tombaugh from Lowell Observatory in Flagstaff, Arizona. Following Pluto's discovery, theories about populations of icy objects like the Kuiper belt, scattered disk, and Oort Cloud that orbit beyond Neptune and could be the source region for comets have been developed.

Since 1992, over 1240 trans-Neptunian objects have been discovered. A few of these have acquired names, such as Chaos, Deucalion, Huya, Ixion, Makemake, Orcus, Quaoar, Rhadamanthus, Sedna, and Varuna. Other, equally interesting objects lack names and are known only by provisional designations like 1992 QB1 which was discovered by David C. Jewitt and Jane X. Luu at the Mauna Kea Observatory as the second discovered TNO since Pluto. Many trans-Neptunian objects are binaries - two bodies with similar masses that orbit each other. Pluto and Charon form one such binary system.

In 2005 a Palomar Observatory-based team led by Mike Brown discovered the first trans-Neptunian object known to be larger than Pluto, Eris (formerly known as 2003 UB313). This discovery caused a fierce debate about the definition of a planet. According to the new definition from the IAU, none of the trans-Neptunian objects is a planet, but four are considered dwarf planets: Pluto, Haumea, Makemake, and Eris.

Table 2.1 contains information about some of the better known trans-Neptunian objects, listed in order of their absolute magnitude. Diameters are only listed if they have been observed through a stellar occultation or through a resolved picture of the object's disk.

Table 2.1: Some of the better known trans-Neptunian objects.

Permanent Name	Provisional Name	Absolute Magnitude	Perihelion [AU]	Aphelion [AU]	Inclination [$\circ$]	Diameter [km]
136199 Eris	2003 UB313	-1.1	38.17	97.61	43.993	$\sim$ 2,400
Pluto	-	-1	30.164	48.494	17.16	2,35050
136472 Makemake	2005 FY9	-0.2	38.666	52.809	29	$\sim$ 1,600
Haumea	2003 EL61	0.1	35.161	51.525	28.2	1,320-1,550
Charon	S/1978 P1	1	30.164	48.494	17.16	1207.2
90377 Sedna	2003 VB12	1.6	76.032	928.048	11.932	$\sim$ 1,600
90482 Orcus	2004 DW	2.3	30.784	48.057	20.6	1,600
50000 Quaoar	2002 LM60	2.6	41.98	45.019	8	1,260 +/- 190
28978 Ixion	2001 KX76	3.2	30.308	49.127	19.6	-
55565	2002 AW197	3.3	-	-	24.4	-

Table 2.1: continued.

Permanent Name	Provisional Name	Absolute Magnitude	Perihelion [AU]	Aphelion [AU]	Inclination [$\circ$]	Diameter [km]
20000 Varuna	2000 WR106	3.7	40.804	45.21	17.2	-
-	2004 XR190	4.5	51.038	63.78	46.735	-
38628 Huya	2000EB173	4.7	28.554	50.95	15.5	-
19521 Chaos	1998 WH24	4.9	40.925	50.376	12.1	-
53311 Deucalion	1999 HU11	6.6	41.579	47.157	0.4	-
38083 Rhadamanthus	1999 HX11	6.7	33.212	45.243	12.7	-
-	1992 QB1	7.2	40.875	46.592	2.2	-

Source: http://www.planetary.org/explore/topics/our_solar_system/trans_neptunian_objects/list.html

Chapter 3

Observations and reductions

The CCD images were taken with a 0.45m f/2.8 remotely-controled telescope located on top of Cerro Burek (Complejo Astronómico el Leoncito, CASLEO) in Argentina, and equipped with a large format CCD camera of 4008 x 2672 pixels. The pixel scale is 1.47 arcsec/pixel and the total FOV of the instrument is 98$\times$65 arcmin. The observations were obtained through a very broad-band filter in order to maximize the signal-to-noise ratio. The transmission curve is shown in Fig. 3.1. Integration times were always 300 s and the telescope was always tracked at sidereal rate. The trailing of the object during these short times was negligible. The observations were taken during 18 nights spanning a period of 33 days. A total of 180 images were acquired for this project. The typical signal-to-noise of the Orcus' observations was around 30. The images were usually taken near the meridian so that the object was at its highest elevation as seen from Cerro Burek; this maximizes the signal-to-noise ratio that can be achieved and at the same time minimizes the differential refraction. Seeing ranged from 2 to 4 arcsec, and therefore the Orcus-Vanth pair was always unresolved.

In each observing night we aimed the telescope at fixed coordinates so that the observed star field was exactly the same at all dates of observations. In other words, the images were not centered on Orcus. A key issue in our program was that the field of view of the instrument is very large, which allowed us to always use the same reference stars for the astrometry. Therefore we could perform very high precision relative astrometry. In other words, our project could be carried out because it was executed with a large FOV instrument. This would not have been possible with the much smaller field of view of most large telescopes.

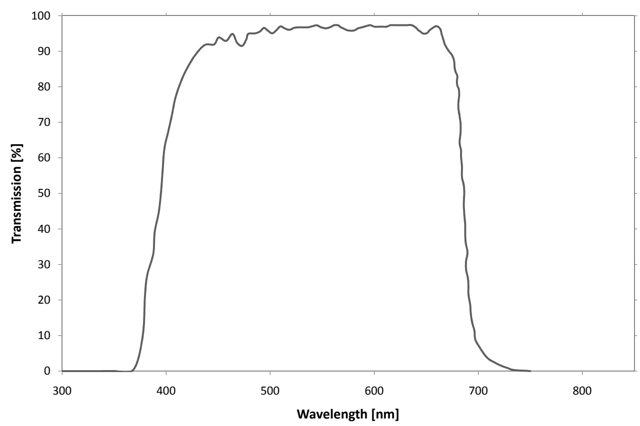

Figure 3.1: Transmission curve of the filter used in this work.

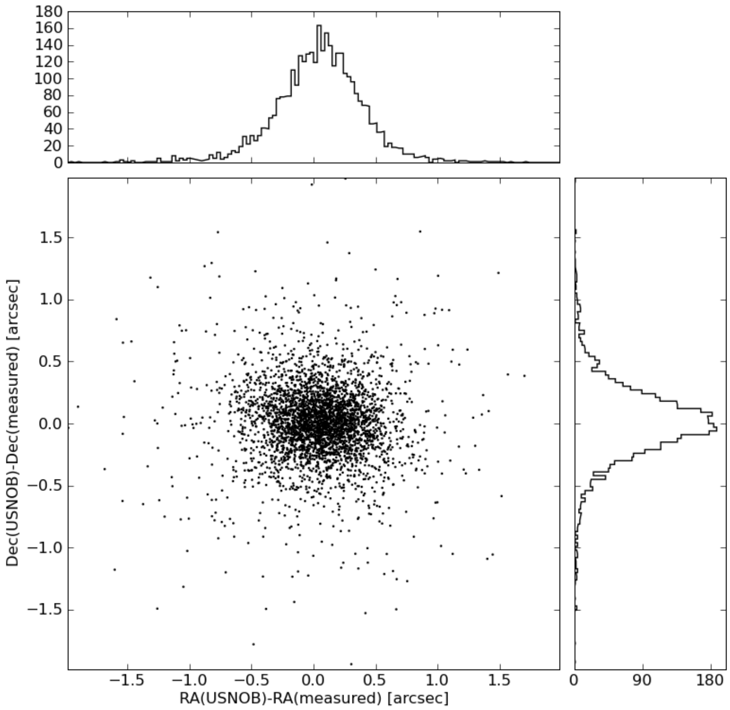

Figure 3.2: The standard deviation of the positions determined for $\sim$ 2000 stars of 18-21mag is 0.18 arcsec.

The images were corrected for bias and dark current by means of master bias and dark current frames obtained by median combining 10 to 20 images on average. Flatfield corrections were also applied with median flatfields taken at dusk. An image of the observed field with the motion of Orcus indicated is presented in Fig. 3.3.

The astrometry was obtained by finding the best third-order polynomial that related the image coordinates and sky coordinates. In order to solve the equations we used $\sim$ 500 UCAC2 reference stars. The UCAC2 astrometric catalog [Zacharias et al., 2004] was used because it offered a convenient number of reference stars in order to solve the plates. However, the choice of the catalog was irrelevant because our goal was to obtain high accuracy relative astrometry, not absolute astrometry. The choice of any other catalog would be acceptable as well, as long as the catalog has enough stars to reliably solve for the polynomial plate constants. The source positions were derived by using SExtractor [Bertin and Arnouts, 1996]. The aperture radius for finding the centroids of the Orcus-Vanth system was 3 pixels. Because the image scale of the detector is 1.47 arcsec/pixel, the 3-pixel aperture guaranteed that most of the flux of the objects entered the aperture even for the poorest seeing conditions possible. The typical uncertainties in the astrometry were slightly larger than a tenth of the pixel size. An average uncertainty of 0.13 arcsec was determined from the measured and known positions of the UCAC2 standars. Nevertheless, because Orcus is fainter than the UCAC2 stars and its centroid determination would be more noisy, we measured the standard deviation of the positions determined for stars of similar brightness to Orcus. The standard deviation turned out to be 0.18 arcsec (shown in fig. 3.2.). Note that these are uncertainties of the individual images. By using large numbers of images one can pinpoint motions smaller than 0.18 arcsec.

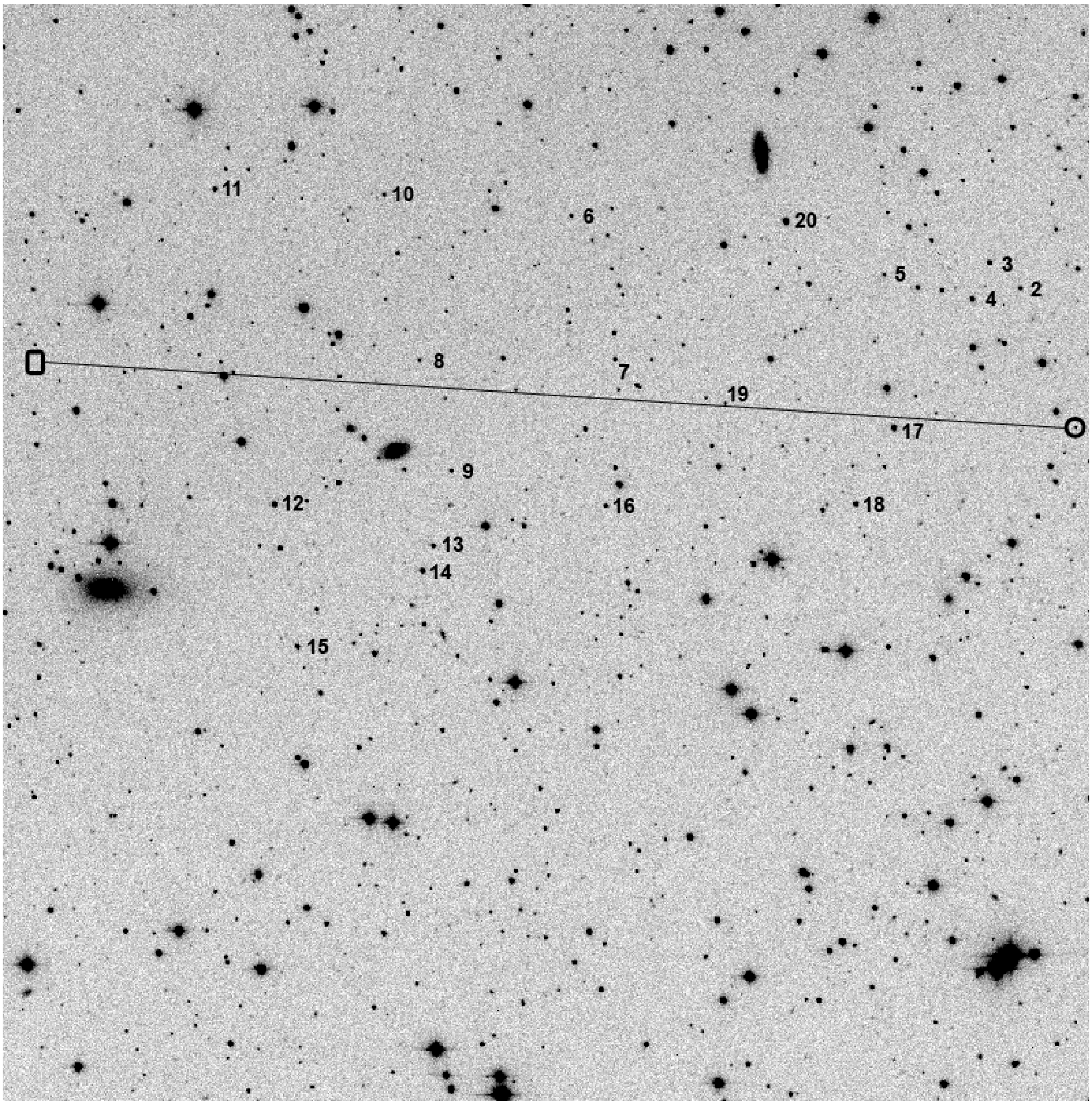

Figure 3.3: Negative image of the central 24.5 $\times$ 24.5 arcmin field that was traversed by Orcus. The position of Orcus at the start of the run is indicated by a circle and its trajectory is shown as a white line. The square indicates where the trajectory ended. North is up, East is to the left. The stars used for the relative photometry analysis are labeled with numbers.

Chapter 4

Results and analysis

Concerning the astrometry results, listed in Table A.1, the right ascension (RA) residuals obtained from an orbital fit to the astrometry are shown in Fig. 4.1. as a function of date. A Lomb periodogram analysis [Lomb, 1976] of the time-series RA residuals is shown in Fig. 4.2. As can be seen in the plot, the highest peak in the periodogram is at 0.1029 cycles/day, which corresponds to a period of 9.7 ± 0.3 days. The confidence level of the detection is well above 99%. Such a period is entirely consistent with the 9.53-day orbital period of Orcus's satellite [Brown et al., 2010]. From a sinusoidal fit, the peak to peak amplitude of the oscillation in the residuals is 0.3 ± 0.2 arcsec.

If most of the orbits of binary systems lie on the ecliptic, we expect that the RA residuals are more appropriate than the declination residuals to study the systems because the declination residuals would

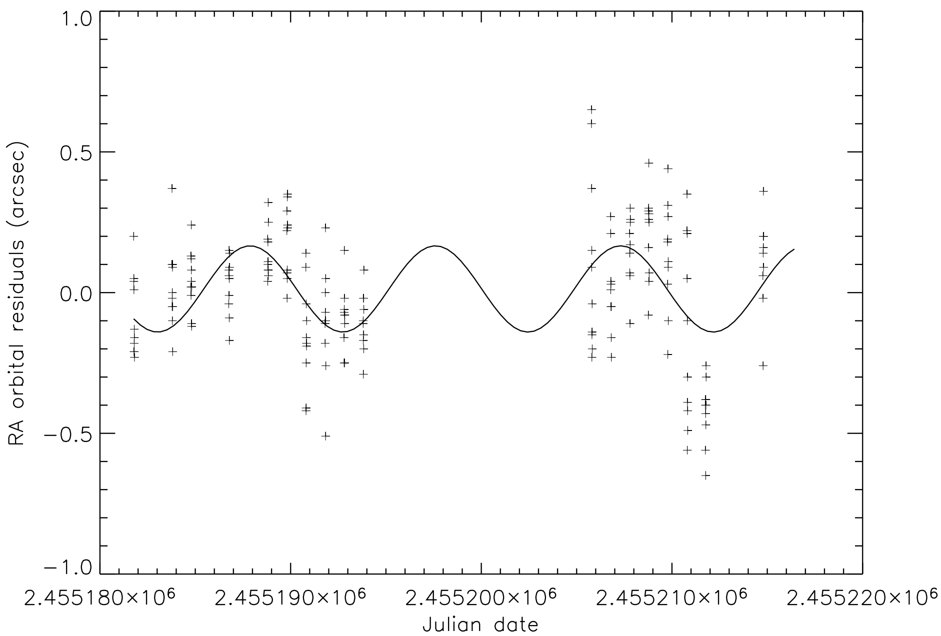

Figure 4.1: Right ascension residuals as a function of date from an orbital fit to the astrometry in Table A.1. A sinusoidal fit to the data is superimposed.

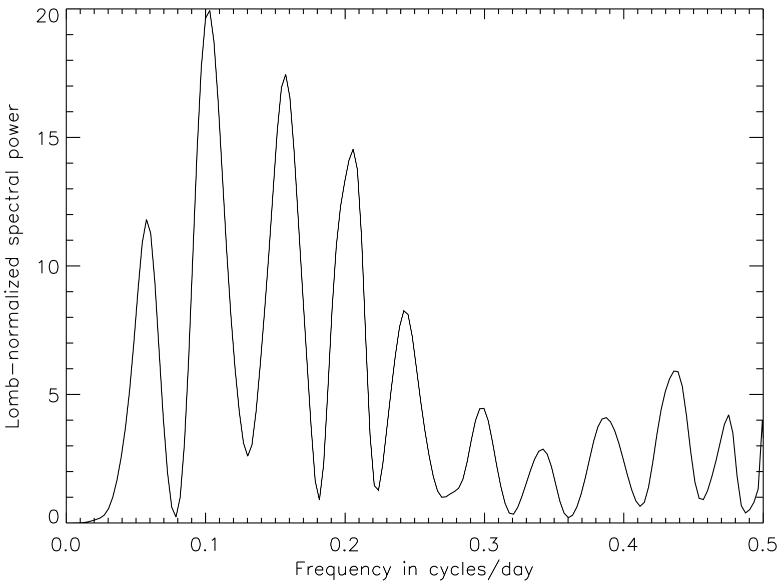

Figure 4.2: Lomb periodogram of the right ascension residuals. The spectral power is plotted as a function of frequency (in cyles/day).

be more difficult to detect in these cases. However, because Vanth's orbit plane appears to be close to the perpendicular to the line of sight, the residuals in declination should also reveal the periodicity. However, we did not find the 9.7-day period. There are several reasons that can explain this. They are discussed in the next section.

We also studied whether the values of the residuals were correlated or not with computed theoretical positions of Orcus' satellite. We did that as a further test to check whether we had indeed detected the presence of a satellite in our data or if the result was a mere coincidence (despite the very high significance level of the detected periodicity). We took nightly averages of the residuals to avoid computing around 200 orbital positions. The binned residuals in arcsec and the theoretical east-west distance of the satellite with respect to Orcus are shown in Table B.1. The theoretical positions were computed with the orbital information given in Brown et al. [2010] and updated in Carry et al. (2010, submitted). A Spearman test results in a clear correlation of the two columns in Table B.1 with a significance level of 97%. We used the Spearman test because this correlation analysis is independent of the exact functional form of the relation, which is not known a priori. Although the angular separation of the satellite with respect to the primary should be linearly related to the theoretical distance between primary and secondary, the photocenter separation in groundbased observations is a complex function of the expected angular separation, seeing, observing conditions, and magnitude difference of the primary to the satellite. Nevertheless we have also performed a linear regression analysis, and the corresponding fit is shown in Fig. 4.3. The coefficients of the fit were 0.003 ± 0.030 for the intercept and $1.39\times10^5 \pm 0.49\times10^5$ for the slope. The periodogram and the correlation analysis are two different diagnostics, and which indicate the presence of astrometry residuals linked to the satellite. We can thus be confident that the presence of Orcus' satellite is unambiguously revealed in our data.

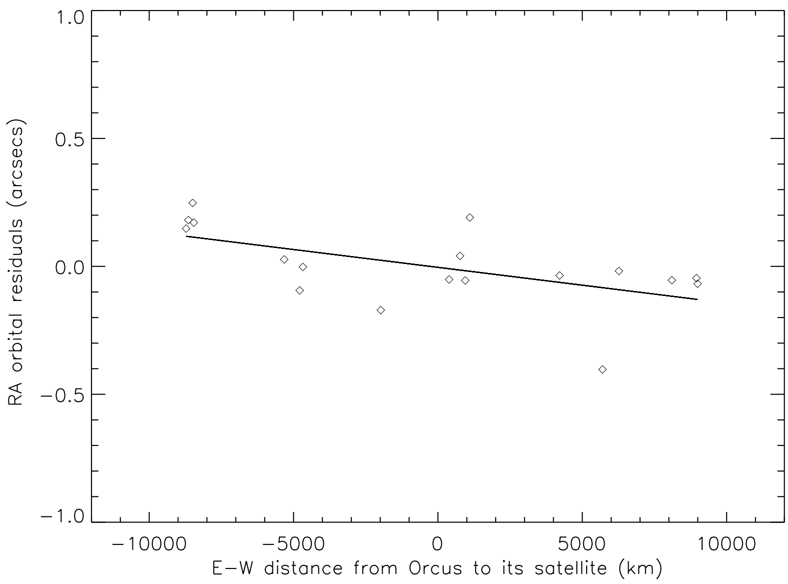

Figure 4.3: Linear fit to the residuals versus computed E-W distance of the secondary to the primary (distance to the East is taken as negative).

Chapter 5

Discussion

The predicted position for Orcus based on its orbit around the Sun should basically correspond to the barycenter of the system, not exactly to that of the largest component of the system. With a nominal mass ratio supposedly of ~ 0.03 (Brown et al. 2010), the offset (primary to center-of-mass) could be $\sim$250km in distance. At Orcus' distance from Earth, and neglecting the light contribution of the secondary, this translates into a mere $\pm$0.009arcsec wobble, which would be undetectable in our data. Therefore, it appears that the light contribution of the secondary must be very relevant.

The maximum separation of Orcus and its satellite is around 9000 km. At Orcus's distance from Earth this translates into approximately 0.3 arcsec. Because the brightness of Orcus' satellite is not negligible, it might shift the photocenter a large enough amount to be detected. Then, the motion of the photocenter around the barycenter (which is very close to the primary) might seem the correct explanation of the periodic signal that we are detecting in our astrometry. We have modeled the maximum photocenter shift of the combined Orcus + satellite system with respect to the primary by generating synthetic images in which there are two point sources with 0.3 arcsec separation and a magnitude difference of 2.5mag [Brown et al., 2010]. These point sources were convolved with Moffat point spread functions (which are typical of ground based observations) for several seeing values, and the position of the photocenter was measured with respect to the position of the primary. The DAOPHOT centroid algorithm was used to find the photocenter. For the typical seeing conditions of our observations the maximum separation of the photocenter with respect to the position of the primary is 0.03 arcsec according to our simulations. Therefore, the peak to peak variation in the residuals of our astrometric observations should be around 0.06 arcsec, which is much larger than the barycenter wobble mentioned in the first paragraph, but 0.06 arcsec is less than the 0.3 ± 0.2 arcsec amplitude of the astrometry residuals that we have measured.

The main parameter to increase the photocenter shift of the simulations to reach the almost 0.3 ± 0.2 arcsec amplitude in the residuals is the magnitude difference between Orcus and its companion. By reducing it to just 0.5mag we would obtain a nearly satisfactory agreement. However, Vanth's brightness would have to oscillate by nearly 2 magnitudes in a rotation period, which is not feasible: the satellite would have to be too elongated. It appears more likely that the true oscillation in the residuals is closer to the lower end of our estimate (0.1 arcsec), which is compatible with the error bar. From the synthetic images, in order to reach 0.1 arcsec amplitude in the residuals, the magnitude difference of secondary to primary should only change from 2.5mag to 2.0mag. This brightness change in the satellite would induce a 0.06mag lightcurve amplitude on the Orcus system. This coincides with the 0.06 ± 0.04 mag lightcurve amplitude published in Ortiz et al. [2011], and therefore the satellite variability might explain both the amplitude of the astrometry residuals and the amplitude of the lightcurve. However, keeping in mind that the orbital plane of the satellite is almost perpendicular to the line of sight, the satellite's spin axis orientation should not be very far from the perpendicular of the orbital plane and in order for a 0.5 mag change to take place with this orientation, the satellite would have to be considerably elongated. A large magnitude change in the satellite' brightness caused by albedo variegations is also a possibility, but high variations are only known for a few objects in the solar system. The saturnian satellite Iapetus, whose leading side is almost 2 magnitudes fainter than its trailing side, is the most extreme case. However, for Orcus it is difficult to envision a similar scenario to that proposed for the existence of Iapetus' two distinct sides. If the real peak to peak amplitude of the RA residuals is even smaller than 0.1 arcsec, then the needed brightness variation of Vanth is smaller than 0.5mag, which would mean that the satellite does not have to be very elongated or present very high albedo variations.

The variability in Vanth can also offer an explanation for the lack of detection of the 9.5 day periodicity in the declination residuals. Because Vath's brightness maxima are nearly in phase with the maxima in RA residuals, the RA residuals are the ones that reach the highest amplitude according to the simulations with synthetic images because the separation is sensitive to the magnitude difference. Other reasons for the lack of detection of 9.5 day periodicity in the declination residuals might be a smaller inclination of the orbital plane than the perpendicular to the line of sight. This might be enough to reduce the amplitude of the residuals so that detectable levels are not reached, or maybe there were systematic effects in declination (like contamination from background stars as Orcus moves with respect to the star field).

From the Orcus experience we can try to draw some conclusions for the prospects of detecting new binaries by means of the astrometric technique and also for the study of known binaries that have very uncertain orbital periods. Because most of the TNO binary discoveries have been made by means of the Hubble Space Telescope or by means of adaptive optic instruments on large telescopes,for which observing time is scarce, a different approach to detect and study binary TNOs that would make use of other more accessible astronomical facilities might boost this important area of TNO science. From the Orcus experience we have detected the satellite with a precision in the relative astrometry measurements of around 0.15 arcsec for the individual exposures. This precision can be considerably reduced with larger telescopes. The main cause for the uncertainties in the relative astrometry is the uncertainty in the centroid calculation, which is basically a function of the achieved signal-to-noise ratio and the pixel scale. Therefore, telescopes in the 2m-range should be capable of delivering good signal to noise ratios on $m_v \sim 21$ objects and would allow us to detect oscillations in the astrometry of only a few tens of mas. This would inturn allow us to detect close faint companions, even closer than the Orcus satellite. Short orbital periods would be the easiest to detect, because mid to long orbital periods would require long observing runs and very large fields of view. Therefore the technique has the potential to reveal closer binaries than those that HST and adaptive optics systems are finding.

Chapter 6

Conclusions

We presented results from an 18-night astrometry run devoted to Orcus' system. The results clearly show that Orcus' satellite imprints an unambiguous periodic signal in the relative astrometry, which is detectable despite the high magnitude difference between Orcus and its satellite (~ 2.5 mag). The periodicity in the astrometry residuals is coincident with the orbital period. The values of the residuals are correlated with the theoretical positions of the satellite with respect to the primary. We have thus shown that detecting binary systems in the trans-Neptunian Belt by means of high-precision astrometry with medium to large telescopes is feasible provided that the barycenter and photocenter of the binary systems do not coincide and are separated by at least tens of milliarcseconds. Because the typical magnitude difference of the binary components is small in the known binaries [Noll et al., 2008], much smaller than in the test case of Orcus, while on the other hand separations of thousands of km are typical among the binary TNOs, the wobble of the photocenter might be detectable. Therefore, specific relative astrometry campaigns with moderately sized telescopes might be a powerful means to study TNOs. Another possible observing strategy is to perform absolute astrometry; this necessitates good astrometric catalogs with faint stars like the astrometric catalog that the Gaia mission will provide.

Chapter 7

Acknowledgements

I'm grateful to Ortiz, J. L. from the Instituto de Astrofisica de Andalucia (IAA-CSIC) who was leading the project and gave me the opportunity to collaborate, to D. Hestroffer who provided Orcus' satellite E-W positions relative to Orcus and N. Morales who did the observations.

Appendix A

Astrometric measurements

Table A.1: Astrometry of the Orcus' system observations, together with the residuals to an orbital fit. The right ascension and declination are referred to epoch J2000

Year	Month	Day (UT)	RA hr	'	"	Dec ^{o}	'	"	RA residual (arcsec)	Dec residual (arcsec)	Δ AU	r AU
2009	12	16.26831	09	49	13.333	-06	29	39.05	+0.16	-0.21	47.463	47.828
2009	12	16.27280	09	49	13.317	-06	29	39.19	+0.05	-0.28	47.463	47.828
2009	12	16.27739	09	49	13.310	-06	29	39.44	+0.07	-0.46	47.463	47.828
2009	12	16.28198	09	49	13.300	-06	29	39.23	+0.05	-0.18	47.463	47.828
2009	12	16.28636	09	49	13.279	-06	29	39.20	-0.14	-0.08	47.463	47.828
2009	12	16.29093	09	49	13.270	-06	29	39.10	-0.15	+0.09	47.463	47.828
2009	12	16.29543	09	49	13.266	-06	29	39.18	-0.08	+0.08	47.463	47.828
2009	12	16.29993	09	49	13.257	-06	29	39.31	-0.09	+0.02	47.463	47.828
2009	12	16.30446	09	49	13.248	-06	29	39.36	-0.09	+0.03	47.462	47.828
2009	12	16.30895	09	49	13.235	-06	29	39.41	-0.16	+0.05	47.462	47.828
2009	12	18.27566	09	49	09.536	-06	30	08.05	+0.10	+0.05	47.433	47.828
2009	12	18.28012	09	49	09.546	-06	30	08.09	+0.38	+0.07	47.433	47.828
2009	12	18.28466	09	49	09.508	-06	30	08.09	-0.05	+0.14	47.433	47.828
2009	12	18.28923	09	49	09.500	-06	30	07.97	-0.03	+0.32	47.432	47.828
2009	12	18.29372	09	49	09.494	-06	30	08.22	+0.01	+0.13	47.432	47.828
2009	12	18.29830	09	49	09.477	-06	30	08.07	-0.10	+0.35	47.432	47.828
2009	12	18.30294	09	49	09.479	-06	30	08.22	+0.07	+0.26	47.432	47.828
2009	12	18.30750	09	49	09.474	-06	30	08.41	+0.13	+0.14	47.432	47.828
2009	12	18.31199	09	49	09.443	-06	30	08.31	-0.19	+0.30	47.432	47.828
2009	12	18.31657	09	49	09.442	-06	30	08.64	-0.07	+0.03	47.432	47.828
2009	12	19.26960	09	49	07.542	-06	30	21.54	-0.01	+0.18	47.418	47.828
2009	12	19.27375	09	49	07.540	-06	30	21.66	+0.09	+0.11	47.418	47.828
2009	12	19.27823	09	49	07.522	-06	30	21.49	-0.04	+0.34	47.418	47.828
2009	12	19.28284	09	49	07.521	-06	30	21.81	+0.09	+0.08	47.418	47.828
2009	12	19.28733	09	49	07.518	-06	30	21.63	+0.19	+0.32	47.418	47.828
2009	12	19.29186	09	49	07.495	-06	30	21.86	-0.01	+0.16	47.417	47.828
2009	12	19.29639	09	49	07.492	-06	30	22.25	+0.08	-0.17	47.417	47.828
2009	12	19.30100	09	49	07.466	-06	30	22.11	-0.16	+0.03	47.417	47.828
2009	12	19.30543	09	49	07.456	-06	30	21.97	-0.17	+0.23	47.417	47.828

Table A.1: continued.

Year	Month	Day	RA			Dec			RA residual	Dec residual	Δ	r
			hr	'	"	o	'	"	(arcsec)	(arcsec)	AU	AU
2009	12	19.30992	09	49	07.458	-06	30	21.96	+0.00	+0.30	47.417	47.828
2009	12	21.25594	09	49	03.355	-06	30	47.10	-0.04	+0.08	47.389	47.828
2009	12	21.26043	09	49	03.354	-06	30	47.07	+0.09	+0.17	47.388	47.828
2009	12	21.26498	09	49	03.346	-06	30	46.88	+0.13	+0.41	47.388	47.828
2009	12	21.26954	09	49	03.328	-06	30	46.97	+0.01	+0.38	47.388	47.828
2009	12	21.27396	09	49	03.331	-06	30	46.88	+0.20	+0.52	47.388	47.828
2009	12	21.27830	09	49	03.301	-06	30	47.21	-0.10	+0.24	47.388	47.828
2009	12	21.28287	09	49	03.301	-06	30	47.23	+0.05	+0.28	47.388	47.828
2009	12	21.28718	09	49	03.276	-06	30	47.59	-0.18	-0.03	47.388	47.828
2009	12	21.29165	09	49	03.286	-06	30	47.40	+0.12	+0.22	47.388	47.828
2009	12	21.29621	09	49	03.275	-06	30	47.44	+0.11	+0.23	47.388	47.828
2009	12	23.29572	09	48	58.781	-06	31	10.72	+0.22	+0.17	47.359	47.828
2009	12	23.30014	09	48	58.762	-06	31	10.70	+0.09	+0.24	47.359	47.828
2009	12	23.30474	09	48	58.752	-06	31	10.95	+0.11	+0.04	47.359	47.828
2009	12	23.30925	09	48	58.746	-06	31	10.94	+0.18	+0.10	47.359	47.828
2009	12	23.31380	09	48	58.731	-06	31	10.97	+0.11	+0.12	47.359	47.828
2009	12	23.31820	09	48	58.720	-06	31	10.95	+0.11	+0.19	47.359	47.828
2009	12	23.32275	09	48	58.722	-06	31	11.13	+0.30	+0.06	47.359	47.828
2009	12	23.32728	09	48	58.697	-06	31	11.03	+0.09	+0.21	47.359	47.828
2009	12	23.33167	09	48	58.684	-06	31	11.10	+0.05	+0.19	47.358	47.828
2009	12	23.33627	09	48	58.687	-06	31	11.11	+0.26	+0.23	47.358	47.828
2009	12	24.30182	09	48	56.393	-06	31	21.86	-0.05	-0.19	47.345	47.828
2009	12	24.30607	09	48	56.407	-06	31	21.62	+0.31	+0.09	47.345	47.828
2009	12	24.31066	09	48	56.382	-06	31	21.61	+0.11	+0.15	47.345	47.828
2009	12	24.31525	09	48	56.362	-06	31	21.75	-0.02	+0.06	47.344	47.828
2009	12	24.31958	09	48	56.358	-06	31	21.73	+0.08	+0.12	47.344	47.828
2009	12	24.32408	09	48	56.349	-06	31	21.79	+0.11	+0.11	47.344	47.828
2009	12	24.32867	09	48	56.352	-06	31	21.67	+0.32	+0.28	47.344	47.828
2009	12	24.33315	09	48	56.338	-06	31	21.67	+0.28	+0.32	47.344	47.828
2009	12	24.33778	09	48	56.333	-06	31	21.78	+0.37	+0.26	47.344	47.828
2009	12	24.34243	09	48	56.312	-06	31	21.89	+0.23	+0.20	47.344	47.828
2009	12	25.29835	09	48	53.990	-06	31	31.52	+0.13	+0.22	47.331	47.828
2009	12	25.30284	09	48	53.985	-06	31	31.89	+0.22	-0.10	47.331	47.828
2009	12	25.30708	09	48	53.936	-06	31	31.86	-0.35	-0.03	47.330	47.828
2009	12	25.31158	09	48	53.924	-06	31	31.86	-0.36	+0.01	47.330	47.828
2009	12	25.31603	09	48	53.921	-06	31	32.11	-0.24	-0.19	47.330	47.828
2009	12	25.32042	09	48	53.922	-06	31	32.26	-0.06	-0.30	47.330	47.828
2009	12	25.32499	09	48	53.903	-06	31	32.35	-0.17	-0.35	47.330	47.828
2009	12	25.32956	09	48	53.889	-06	31	32.36	-0.20	-0.31	47.330	47.828
2009	12	25.33417	09	48	53.878	-06	31	32.24	-0.19	-0.15	47.330	47.828
2009	12	25.33866	09	48	53.871	-06	31	32.38	-0.13	-0.24	47.330	47.828
2009	12	26.30547	09	48	51.464	-06	31	41.61	-0.13	-0.29	47.317	47.828
2009	12	26.31010	09	48	51.449	-06	31	41.52	-0.17	-0.16	47.316	47.828
2009	12	26.31459	09	48	51.442	-06	31	41.65	-0.10	-0.25	47.316	47.828
2009	12	26.31914	09	48	51.436	-06	31	41.78	-0.02	-0.34	47.316	47.828

Table A.1: continued.

Year	Month	Day	RA			Dec			RA residual	Dec residual	Δ	r
			hr	’	”	^{o}	’	”	(arcsec)	(arcsec)	AU	AU
2009	12	26.32366	09	48	51.418	-06	31	41.77	-0.11	-0.29	47.316	47.828
2009	12	26.32818	09	48	51.429	-06	31	41.78	+0.23	-0.26	47.316	47.828
2009	12	26.33277	09	48	51.367	-06	31	42.10	-0.52	-0.53	47.316	47.828
2009	12	26.33739	09	48	51.391	-06	31	41.72	+0.02	-0.11	47.316	47.828
2009	12	26.34193	09	48	51.370	-06	31	41.81	-0.12	-0.16	47.316	47.828
2009	12	26.34652	09	48	51.344	-06	31	41.97	-0.33	-0.28	47.316	47.828
2009	12	27.29975	09	48	48.920	-06	31	50.57	-0.16	-0.41	47.303	47.828
2009	12	27.30432	09	48	48.903	-06	31	50.60	-0.23	-0.40	47.303	47.828
2009	12	27.30880	09	48	48.899	-06	31	50.55	-0.11	-0.31	47.303	47.828
2009	12	27.31334	09	48	48.891	-06	31	50.78	-0.05	-0.50	47.303	47.828
2009	12	27.31786	09	48	48.893	-06	31	50.59	+0.16	-0.27	47.303	47.828
2009	12	27.32250	09	48	48.868	-06	31	51.12	-0.03	-0.76	47.303	47.828
2009	12	27.32697	09	48	48.852	-06	31	50.61	-0.09	-0.21	47.302	47.828
2009	12	27.33153	09	48	48.829	-06	31	50.99	-0.26	-0.55	47.302	47.828
2009	12	27.33610	09	48	48.825	-06	31	50.74	-0.13	-0.26	47.302	47.828
2009	12	27.34054	09	48	48.816	-06	31	51.09	-0.09	-0.57	47.302	47.828
2009	12	28.30215	09	48	46.290	-06	31	58.81	-0.18	-0.33	47.289	47.828
2009	12	28.30668	09	48	46.277	-06	31	58.80	-0.19	-0.28	47.289	47.828
2009	12	28.31124	09	48	46.263	-06	31	58.94	-0.21	-0.39	47.289	47.828
2009	12	28.31578	09	48	46.243	-06	31	59.02	-0.33	-0.43	47.289	47.828
2009	12	28.32019	09	48	46.249	-06	31	58.84	-0.06	-0.22	47.289	47.828
2009	12	28.32471	09	48	46.228	-06	31	58.89	-0.19	-0.23	47.289	47.828
2009	12	28.32923	09	48	46.224	-06	31	59.05	-0.07	-0.35	47.289	47.828
2009	12	28.33380	09	48	46.199	-06	31	59.00	-0.25	-0.27	47.289	47.828
2009	12	28.33814	09	48	46.196	-06	31	59.04	-0.12	-0.27	47.289	47.828
2009	12	28.34268	09	48	46.193	-06	31	59.02	+0.02	-0.22	47.289	47.828
2010	01	09.27728	09	48	10.230	-06	32	49.95	+0.47	+0.39	47.140	47.828
2010	01	09.28180	09	48	10.226	-06	32	50.14	+0.64	+0.20	47.140	47.828
2010	01	09.28628	09	48	10.192	-06	32	49.92	+0.36	+0.42	47.140	47.828
2010	01	09.29086	09	48	10.165	-06	32	50.28	+0.19	+0.06	47.140	47.828
2010	01	09.29541	09	48	10.151	-06	32	50.22	+0.21	+0.13	47.140	47.828
2010	01	09.29985	09	48	10.116	-06	32	50.53	-0.08	-0.18	47.140	47.828
2010	01	09.30438	09	48	10.099	-06	32	50.28	-0.11	+0.07	47.140	47.828
2010	01	09.30893	09	48	10.083	-06	32	50.34	-0.11	+0.02	47.140	47.828
2010	01	09.31342	09	48	10.074	-06	32	50.23	-0.02	+0.13	47.140	47.828
2010	01	09.31801	09	48	10.049	-06	32	50.24	-0.16	+0.12	47.140	47.828
2010	01	10.28184	09	48	06.814	-06	32	50.63	+0.12	+0.04	47.129	47.828
2010	01	10.28644	09	48	06.789	-06	32	51.18	-0.01	-0.51	47.129	47.828
2010	01	10.29102	09	48	06.775	-06	32	50.58	+0.02	+0.09	47.129	47.828
2010	01	10.29558	09	48	06.758	-06	32	50.72	+0.00	-0.05	47.129	47.828
2010	01	10.30008	09	48	06.745	-06	32	50.34	+0.04	+0.33	47.129	47.828
2010	01	10.30462	09	48	06.723	-06	32	50.55	-0.05	+0.12	47.129	47.828
2010	01	10.30909	09	48	06.706	-06	32	50.48	-0.08	+0.19	47.129	47.828
2010	01	10.31362	09	48	06.684	-06	32	50.47	-0.17	+0.20	47.129	47.828
2010	01	10.31815	09	48	06.677	-06	32	50.58	-0.04	+0.09	47.129	47.828

Table A.1: continued.

Year	Month	Day	RA			Dec			RA residual	Dec residual	Δ	r
			hr	’	”	o	’	”	(arcsec)	(arcsec)	AU	AU
2010	01	10.32258	09	48	06.658	-06	32	50.56	-0.09	+0.11	47.128	47.828
2010	01	11.27892	09	48	03.401	-06	32	50.26	+0.19	+0.13	47.118	47.828
2010	01	11.28336	09	48	03.384	-06	32	50.19	+0.17	+0.20	47.118	47.828
2010	01	11.28785	09	48	03.361	-06	32	50.10	+0.07	+0.29	47.118	47.828
2010	01	11.29245	09	48	03.349	-06	32	50.04	+0.13	+0.34	47.118	47.828
2010	01	11.29683	09	48	03.329	-06	32	50.17	+0.06	+0.21	47.118	47.828
2010	01	11.30130	09	48	03.303	-06	32	50.39	-0.09	-0.01	47.118	47.828
2010	01	11.30579	09	48	03.307	-06	32	50.17	+0.20	+0.21	47.118	47.828
2010	01	11.31043	09	48	03.295	-06	32	50.50	+0.27	-0.13	47.118	47.828
2010	01	11.31486	09	48	03.277	-06	32	50.11	+0.23	+0.26	47.118	47.828
2010	01	11.31930	09	48	03.263	-06	32	50.17	+0.26	+0.20	47.118	47.828
2010	01	12.26323	09	47	59.959	-06	32	49.52	-0.12	-0.01	47.107	47.828
2010	01	12.26767	09	47	59.964	-06	32	49.48	+0.19	+0.03	47.107	47.828
2010	01	12.27218	09	47	59.939	-06	32	49.50	+0.06	+0.00	47.107	47.828
2010	01	12.27659	09	47	59.936	-06	32	49.60	+0.25	-0.10	47.107	47.828
2010	01	12.28107	09	47	59.918	-06	32	49.63	+0.22	-0.14	47.107	47.828
2010	01	12.28548	09	47	59.914	-06	32	49.48	+0.40	+0.01	47.107	47.828
2010	01	12.29011	09	47	59.886	-06	32	49.26	+0.22	+0.22	47.107	47.828
2010	01	12.29460	09	47	59.853	-06	32	49.43	-0.03	+0.05	47.107	47.828
2010	01	12.29904	09	47	59.852	-06	32	49.09	+0.19	+0.38	47.107	47.828
2010	01	12.30352	09	47	59.824	-06	32	49.58	+0.01	-0.11	47.107	47.828
2010	01	13.26833	09	47	56.432	-06	32	48.00	+0.12	+0.00	47.097	47.828
2010	01	13.27293	09	47	56.405	-06	32	48.06	-0.04	-0.07	47.097	47.828
2010	01	13.27753	09	47	56.397	-06	32	48.14	+0.09	-0.15	47.097	47.828
2010	01	13.28210	09	47	56.353	-06	32	47.80	-0.32	+0.18	47.097	47.828
2010	01	13.28664	09	47	56.373	-06	32	47.93	+0.23	+0.04	47.097	47.828
2010	01	13.29116	09	47	56.366	-06	32	47.93	+0.36	+0.03	47.097	47.828
2010	01	13.29566	09	47	56.337	-06	32	47.80	+0.17	+0.15	47.097	47.828
2010	01	13.30027	09	47	56.308	-06	32	47.60	-0.01	+0.35	47.097	47.828
2010	01	13.30488	09	47	56.293	-06	32	48.00	+0.02	-0.06	47.097	47.828
2010	01	13.30932	09	47	56.263	-06	32	48.03	-0.19	-0.10	47.097	47.828
2010	01	14.28568	09	47	52.794	-06	32	45.95	+0.07	-0.11	47.087	47.828
2010	01	14.29017	09	47	52.786	-06	32	45.76	+0.20	+0.07	47.086	47.828
2010	01	14.29460	09	47	52.760	-06	32	45.59	+0.05	+0.23	47.086	47.828
2010	01	14.29903	09	47	52.756	-06	32	45.63	+0.23	+0.18	47.086	47.828
2010	01	14.30353	09	47	52.703	-06	32	45.75	-0.31	+0.05	47.086	47.828
2010	01	14.30790	09	47	52.736	-06	32	45.37	+0.42	+0.42	47.086	47.828
2010	01	14.31242	09	47	52.680	-06	32	45.70	-0.17	+0.08	47.086	47.828
2010	01	14.31687	09	47	52.668	-06	32	45.99	-0.11	-0.22	47.086	47.828
2010	01	14.32121	09	47	52.642	-06	32	45.96	-0.26	-0.21	47.086	47.828
2010	01	14.32564	09	47	52.623	-06	32	45.57	-0.30	+0.17	47.086	47.828
2010	01	15.25154	09	47	49.283	-06	32	43.37	-0.23	-0.17	47.077	47.828
2010	01	15.25608	09	47	49.252	-06	32	43.00	-0.44	+0.19	47.077	47.828
2010	01	15.26066	09	47	49.243	-06	32	43.23	-0.32	-0.05	47.077	47.828
2010	01	15.26521	09	47	49.224	-06	32	43.16	-0.36	+0.00	47.077	47.828

Table A.1: continued.

Year	Month	Day	RA			Dec			RA residual	Dec residual	Δ	r
			hr	’	”	*o*	’	”	(arcsec)	(arcsec)	AU	AU
2010	01	15.26968	09	47	49.192	-06	32	43.33	-0.59	-0.18	47.077	47.828
2010	01	15.27425	09	47	49.193	-06	32	43.05	-0.32	+0.09	47.077	47.828
2010	01	15.27873	09	47	49.171	-06	32	43.03	-0.40	+0.09	47.077	47.828
2010	01	15.28308	09	47	49.160	-06	32	43.09	-0.32	+0.02	47.077	47.828
2010	01	15.28765	09	47	49.149	-06	32	43.12	-0.23	-0.03	47.076	47.828
2010	01	15.29215	09	47	49.131	-06	32	43.06	-0.25	+0.02	47.076	47.828
2010	01	18.27056	09	47	38.125	-06	32	31.26	+0.06	+0.05	47.048	47.828
2010	01	18.27514	09	47	38.103	-06	32	31.21	+0.00	+0.07	47.048	47.828
2010	01	18.27968	09	47	38.069	-06	32	31.32	-0.25	-0.06	47.048	47.828
2010	01	18.28411	09	47	38.080	-06	32	31.48	+0.17	-0.24	47.048	47.828
2010	01	18.28857	09	47	38.063	-06	32	31.24	+0.17	-0.02	47.048	47.828
2010	01	18.29304	09	47	38.044	-06	32	31.86	+0.14	-0.66	47.048	47.828
2010	01	18.29760	09	47	38.037	-06	32	31.43	+0.29	-0.26	47.048	47.828
2010	01	18.30224	09	47	38.006	-06	32	31.33	+0.10	-0.18	47.048	47.828
2010	01	18.30683	09	47	37.993	-06	32	31.15	+0.17	-0.02	47.048	47.828
2010	01	18.31138	09	47	37.962	-06	32	31.47	-0.04	-0.36	47.048	47.828

Appendix B

Vanth's positions relative to Orcus

Table B.1: Orcus' satellite E-W positions relative to Orcus (negative to the East) as a function of date and the RA average residuals for the listed mean julian dates.

Julian Date	E-W Distance (km)	RA residuals (arcsec)
2455181.78865	-1979.31	-0.171
2455183.79607	8104.50	-0.054
2455184.78963	8956.02	-0.046
2455186.77611	767.11	0.041
2455188.81598	-8642.56	0.181
2455189.82195	-8496.13	0.248
2455190.81837	-4788.64	-0.094
2455191.82597	946.28	-0.055
2455192.82017	6269.45	-0.018
2455193.82246	8996.14	-0.068
2455205.79762	1106.78	0.191
2455206.80230	-4675.49	-0.002
2455207.79911	-8455.05	0.171
2455208.78335	-8722.25	0.148
2455209.78888	-5322.47	0.027
2455210.80571	387.32	-0.051
2455211.77190	5701.46	-0.403
2455214.78864	4213.96	-0.036

Bibliography

M. A. Barucci, F. Merlin, A. Guilbert, C. de Bergh, A. Alvarez-Candal, O. Hainaut, A. Doressoundiram, C. Dumas, T. Owen, and A. Coradini. Surface composition and temperature of the TNO Orcus. *Astronomy and Astrophysics*, 479:L13–L16, February 2008. doi: 10.1051/0004-6361:20079079.

P. G. Benavidez and A. Campo Bagatin. Collisional evolution of Trans-Neptunian populations: Effects of fragmentation physics and estimates of the abundances of gravitational aggregates. *Planetary Space Science*, 57:201–215, February 2009. doi: 10.1016/j.pss.2008.09.007.

E. Bertin and S. Arnouts. SExtractor: Software for source extraction. *Astronomy and Astrophysics,Suppl.*, 117:393–404, June 1996.

M. E. Brown, D. Ragozzine, J. Stansberry, and W. C. Fraser. The Size, Density, and Formation of the Orcus-Vanth System in the Kuiper Belt. *Astronomical Journal*, 139:2700–2705, June 2010. doi: 10.1088/0004-6256/139/6/2700.

D. R. Davis and P. Farinella. Collisional Evolution of Edgeworth-Kuiper Belt Objects. *Icarus*, 125: 50–60, January 1997. doi: 10.1006/icar.1996.5595.

C. de Bergh, A. Delsanti, G. P. Tozzi, E. Dotto, A. Doressoundiram, and M. A. Barucci. The surface of the transneptunian object 90482 Orcus. *Astronomy and Astrophysics*, 437:1115–1120, July 2005. doi: 10.1051/0004-6361:20042533.

J. A. Fernandez. On the existence of a comet belt beyond Neptune. *Monthly Notices of the RAS*, 192: 481–491, August 1980.

S. Fornasier, E. Dotto, M. A. Barucci, and C. Barbieri. Water ice on the surface of the large TNO 2004 DW. *Astronomy and Astrophysics*, 422:L43–L46, July 2004. doi: 10.1051/0004-6361:20048004.

R. Gomes, H. F. Levison, K. Tsiganis, and A. Morbidelli. Origin of the cataclysmic Late Heavy Bombardment period of the terrestrial planets. *Nature*, 435:466–469, May 2005. doi: 10.1038/nature03676.

T. L. Lim, J. Stansberry, T. G. Müller, M. Mueller, E. Lellouch, C. Kiss, P. Santos-Sanz, E. Vilenius, S. Protopapa, R. Moreno, A. Delsanti, R. Duffard, S. Fornasier, O. Groussin, A. W. Harris, F. Henry, J. Horner, P. Lacerda, M. Mommert, J. L. Ortiz, M. Rengel, A. Thirouin, D. Trilling, A. Barucci, J. Crovisier, A. Doressoundiram, E. Dotto, P. J. Gutiérrez Buenestado, O. Hainaut, P. Hartogh, D. Hestroffer, M. Kidger, L. Lara, B. M. Swinyard, and N. Thomas. "TNOs are Cool": A survey of the trans-Neptunian region . III. Thermophysical properties of 90482 Orcus and 136472 Makemake. *Astronomy and Astrophysics*, 518:L148, July 2010. doi: 10.1051/0004-6361/201014701.

N. R. Lomb. Least-squares frequency analysis of unequally spaced data. *Astrophysics and Space Science*, 39:447–462, February 1976. doi: 10.1007/BF00648343.

A. Morbidelli, H. F. Levison, K. Tsiganis, and R. Gomes. Chaotic capture of Jupiter's Trojan asteroids in the early Solar System. *Nature*, 435:462–465, May 2005. doi: 10.1038/nature03540.

K. S. Noll, W. M. Grundy, E. I. Chiang, J.-L. Margot, and S. D. Kern. *Binaries in the Kuiper Belt*, pages 345–363. 2008.

J. L. Ortiz, P. J. Gutiérrez, P. Santos-Sanz, V. Casanova, and A. Sota. Short-term rotational variability of eight KBOs from Sierra Nevada Observatory. *Astronomy and Astrophysics*, 447:1131–1144, March 2006. doi: 10.1051/0004-6361:20053572.

J. L. Ortiz, A. Cikota, S. Cikota, D. Hestroffer, A. Thirouin, N. Morales, R. Duffard, R. Gil-Hutton, P. Santos-Sanz, and I. de La Cueva. A mid-term astrometric and photometric study of trans-Neptunian object (90482) Orcus. *Astronomy and Astrophysics*, 525:A31, January 2011. doi: 10.1051/0004-6361/201015309.

S. S. Sheppard. Light Curves of Dwarf Plutonian Planets and other Large Kuiper Belt Objects: Their Rotations, Phase Functions, and Absolute Magnitudes. *Astronomical Journal*, 134:787–798, August 2007. doi: 10.1086/519072.

J. Stansberry, W. Grundy, M. Brown, D. Cruikshank, J. Spencer, D. Trilling, and J.-L. Margot. *Physical Properties of Kuiper Belt and Centaur Objects: Constraints from the Spitzer Space Telescope*, pages 161–179. 2008.

S. C. Tegler, W. Romanishin, G. J. Consolmagno, J. Rall, R. Worhatch, M. Nelson, and S. Weidenschilling. The period of rotation, shape, density, and homogeneous surface color of the Centaur 5145 Pholus. *Icarus*, 175:390–396, June 2005. doi: 10.1016/j.icarus.2004.12.011.

A. Thirouin, J. L. Ortiz, R. Duffard, P. Santos-Sanz, F. J. Aceituno, and N. Morales. Short-term variability of a sample of 29 trans-Neptunian objects and Centaurs. *Astronomy and Astrophysics*, 522: A93, November 2010. doi: 10.1051/0004-6361/200912340.

C. A. Trujillo, M. E. Brown, D. L. Rabinowitz, and T. R. Geballe. Near-Infrared Surface Properties of the Two Intrinsically Brightest Minor Planets: (90377) Sedna and (90482) Orcus. *Astrophysical Journal*, 627:1057–1065, July 2005. doi: 10.1086/430337.

K. Tsiganis, R. Gomes, A. Morbidelli, and H. F. Levison. Origin of the orbital architecture of the giant planets of the Solar System. *Nature*, 435:459–461, May 2005. doi: 10.1038/nature03539.

N. Zacharias, S. E. Urban, M. I. Zacharias, G. L. Wycoff, D. M. Hall, D. G. Monet, and T. J. Rafferty. The Second US Naval Observatory CCD Astrograph Catalog (UCAC2). *Astronomical Journal*, 127: 3043–3059, May 2004. doi: 10.1086/386353.